Nickel-Based Superalloy Operating Temperature Determination via Analysis of Gamma/Gamma' Microstructure and Coating/Base Material Interdiffusion

by

Wendy D. Ham

Submitted to the Department of Materials Science and Engineering
in partial fulfillment of the requirements for the degree of

Master of Science in Materials Science and Engineering

at the

MASSACHUSETTS INSTITUTE OF TECHNOLOGY

June 2005

Author .....
Department of Materials Science and Engineering
February 2005

Certified by .....
Samuel M. Allen
POSCO Professor of Physical Metallurgy
Thesis Supervisor

Accepted by .....
Gerbrand Ceder
R.P. Simmons Professor of Materials Science and Engineering
Chairman, Department Committee on Graduate Students

Nickel-Based Superalloy Operating Temperature Determination via Analysis of Gamma/Gamma′ Microstructure and Coating/Base Material Interdiffusion

by

Wendy D. Ham

Submitted to the Department of Materials Science and Engineering
on February 2005, in partial fulfillment of the
requirements for the degree of
Master of Science in Materials Science and Engineering

Abstract

The average operating temperature of RENÉ N5® high pressure turbine blades was evaluated via γ/γ' microstructure and coating/base metal interdiffusion methods. The γ' volume fraction was measured by point counting and direct area measurement. The data, however, were found inadequate to accurately determine the operating temperature. The interdiffusion between the platinum aluminide coating and the base material was modeled with an error function solution to Fick's Second Law. This method provided an estimation of the operating temperature that varied from the reported operating temperature by only 1%.

Thesis Supervisor: Samuel M. Allen
Title: POSCO Professor of Physical Metallurgy

Acknowledgments

My thanks go out to:

My thesis adviser, Professor Samuel Allen, who has been pivotal in my effort to complete this thesis.

GE Aircraft Engines, William Crawford, and all my coworkers in the Thomson Materials Lab for their guidance during my time there.

Joseph Dhosi and Kathleen Farrell for their help navigating the Institvte.

My parents for their unflagging support as I pursued my goals.

And my husband, Doug, for all his love, encouragement and help with typing and editing.

Contents

List of Figures

List of Tables

Introduction

In jet engines, the high pressure turbine blades harness energy from the combusted core flow of gas to power the compression of the intake air [17]. **(Figure 1)** The high pressure turbine (HPT) blades **(Figure 2)** are assembled into a turbine wheel **(Figure 3)** which is housed in the turbine shroud. The efficiency with which the turbine harnesses energy is governed by many factors including the clearance between the blade tips and the turbine shroud. The larger the clearance, the more air bypasses the turbine blades; when the blades touch the turbine shroud, however, large amounts of friction and heat are generated and the tips of the blades are damaged. With a proper clearance, the turbine wheel can harness enough energy to rotate at over 40,000 RPM [3]. This rotation causes a centrifically generated radial force on the blades [19].

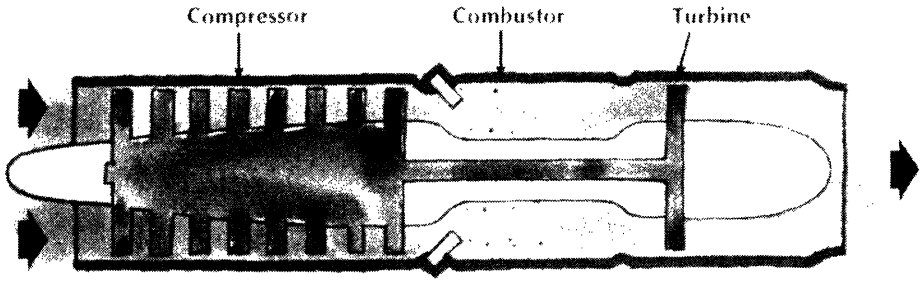

Figure 1: The turbine wheel harnesses energy with which to rotate the compressor [4, page 39]

Along with being in a high-stress environment, the HPT blades also see very high temperatures and broad temperature cycling. With the engine at full-power air leaving the combustor can be as hot as 2273 K [12]. The turbine blades can not withstand that temperature, though, so ambient-temperature air is brought in and mixed with the combusted gases before they reach the turbine. Even after this mixing, the operating temperature in the turbine, T4.5, can be as high as 1273 K [12]. Exposure to this high temperature for prolonged periods of time can lead to oxidation of a blade's surface. Sulfidation can also occur in certain environments such as humid salty air over the ocean or acid rain. Operating in this high-stress, high-temperature environment puts great demands on the strength of the HPT blades and requires that

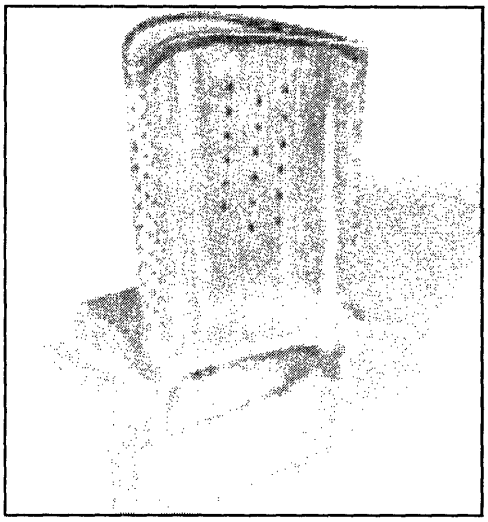

Figure 2: A representative high pressure turbine blade [5]

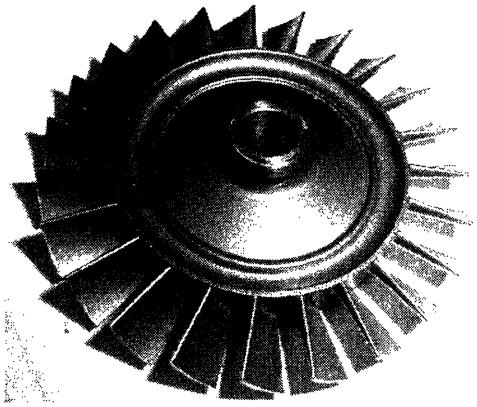

Figure 3: Bladed Disk Similar to a Turbine Wheel [20]

they be made from specialty materials.

Nickel-based superalloys are technologically advanced materials designed to have superior strength and creep resistance at elevated temperatures. For this reason, HPT blades are often made of directionally-solidified, single-crystal, Ni-based superalloys [6]. The most important strengthening mechanism in this type of material is the two-phase equilibrium microstructure of gamma prime (γ') within a matrix of gamma (γ) phase [3]. To protect the HPT blades from their harsh environment, high-performance coatings, often platinum-aluminide, are applied to many blades. These coatings resist the oxidation and sulfidation that are possible [6].

As the blades operate, however, the distribution of elements in the coating and adjacent base metal, as well as the γ/γ' microstructure, undergo significant changes. The microstructure changes as the γ' coarsens, changing size and shape. There is also an overall reduction in the amount of γ' in the structure as long as the temperature is increasing. After being held at a given temperature, however, the volume fraction will remain constant as long as the blades are held at that temperature or below. Another change that occurs in such a high-temperature environment is extensive interdiffusion of coating and base material elements [2].

As HPT blades are held at high temperatures during flight, they begin to lose

their strength and creep resistance. The γ/γ' structure coarsens and interdiffusion weakens the coating. This allows the blade's average temperature to be estimated based on the extent to which these effects are seen. This thesis analyzes the accuracy to which the average running temperature can be calculated via either of the two methods: γ' volume fraction or the extent of base material and coating interdiffusion.

This research was performed at GE Aircraft Engines in Lynn, MA. The HPT blades were from a GE commercial engine and were made of RENÉ N5® superalloy with platinum aluminide coating. All testing was done on an engine running in an indoor factory test cell. Engine cycling followed typical commercial patterns and the average bulk metal temperature was 1393 K. Blades were analyzed before running, after 1891 hours and again after 10500 hours, both metallographically and via scanning electron microscopy (SEM).

Gamma/Gamma′ Two Phase Microstructure

Background

Nickel-based superalloys rely heavily on a two-phase γ' in γ microstructure in order to maintain high creep resistance at elevated temperatures. The γ phase, which forms the matrix of the base material, has a face-centered cubic structure as seen in **Figure 4**. Ideally, to achieve maximum strengthening, this matrix would be filled with a fine dispersion of cuboidal γ' precipitates. Unlike γ, γ' forms a primitive cubic structure **(Figure 5)**; within the unit cell lie three whole Ni atoms (six halves) and one Al atom (eight eighths). Therefore, γ' alloys take the approximate form of Ni_3X, where X is often Al, Pt, or Ti. The phase is not, however, strictly stoichiometric as X sites may be filled by Ni or vice versa [2].

While the γ/γ' two-phase microstructure is at meta-stable equilibrium while at room temperature, as it is held at elevated temperatures it begins to coarsen. At higher temperatures, the γ structure can hold more of the X element in suspension and this leads to reduced γ' volume fraction. Lacking the fine precipitate structure,

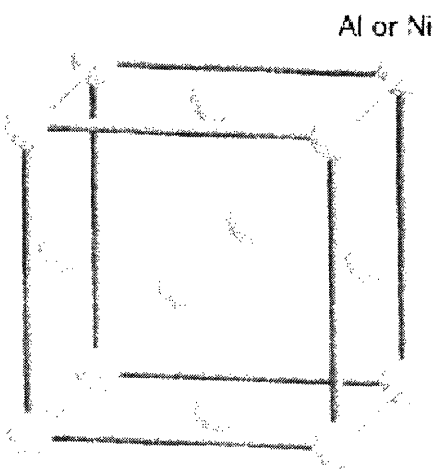

Figure 4: The face-centered cubic crystal structure of γ phase [2]

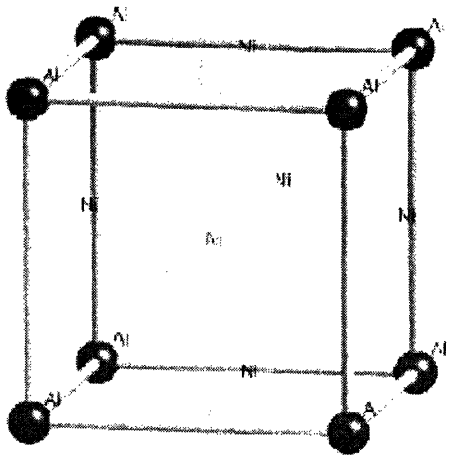

Figure 5: The primitive cubic crystal structure of γ' phase [2]

the material begins to lose its creep resistance. By measuring the γ' volume fraction, it is possible to estimate the average temperature that the superalloy experienced.

Materials and Methods

This research was performed on HPT blades made of RENÉ N5® **(Table 1)** nickel-based superalloy. After operating for various lengths of time in a test engine, cross sections of the blades were mounted in CONDUCTOMET conductive mount media in order to examine the trailing edge sections of the blades. The trailing edges were chosen for study because they would have been expected to have seen higher temperatures than any other locations within the blade. The mounts were then polished and etched using standard metallographic procedures (details withheld - proprietary information).

Scanning electron microscopy (SEM) was used to examine the γ' structure in each of the sections. **Figure 6** shows the microstructure in the blades before they were run; the darker cuboidal phase is the γ', and the lighter matrix is the γ. The larger blurred regions which are on the order of a half micron across by several microns tall are γ sheets which are γ phase oriented perpendicularly to the plane of the microphotos. SEM images were taken of not-yet-run material as well as the microstructure after

RENÉ N5 Composition	
Element	Weight %
Ni	63.09%
Co	7.50%
Cr	7.00%
Ta	6.50%
Al	6.20%
W	5.00%
Re	3.00%
Mo	1.50%
Hf	0.15%
Co	0.05%
B	0.004%

Table 1: RENÉ N5® elemental composition [11]

1891 hours and 10500 hours.

Two methods were used in order to evaluate the γ' volume fraction in the SEM images. The first method was the point counting method. This method takes advantage of the fact that in a solid made of un-aligned particles, the point fraction of a given phase seen in a two-dimensional random cross-section is equal to the volume fraction of that phase in the three-dimensional solid. While the initial microstructure seen in the unrun blade does show alignment, it can be assumed that if the grid is laid mismatched to any symmetry the point fraction will still correlate well to the volume fraction. The point fraction is found by laying a grid of test points randomly across the image and counting the number of the grid points that fall within the phase of interest. In this case, a grid was laid onto the SEM image **(Figure 7)** and the number of intersections that fell in the dark γ' grains was counted. Intersections that appeared to fall on γ/γ' boundaries were counted as a half. The number of γ' points was divided by the total 396 intersections to determine the γ' volume fraction.

The second method used to measure γ' volume fraction was direct measurement of the area of the γ' grains in the SEM images. Using a freeware program, UTHSCSA (University of Texas Health Science Center at San Antonio) Image Tool [13], the SEM image was analyzed and a bimodal histogram of grey scale values present in the image was created. The edges of the γ' grains were found by manually setting a threshold

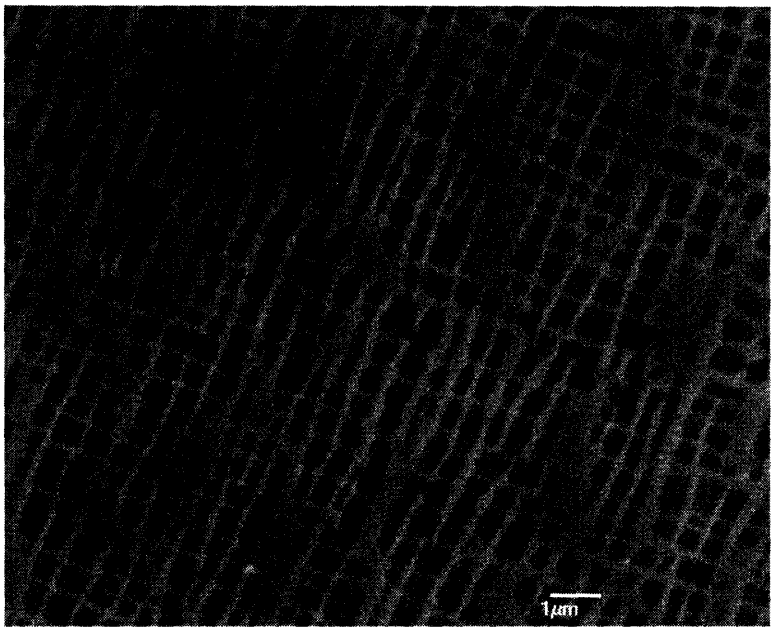

Figure 6: Two-phase γ/γ' microstructure in unrun RENÉ N5® HPT blade

grey scale which separated the dark and light areas of the image. **(Figure 8)** The program could then measure the area of each γ' grain as well as the area of the entire image. By summing the areas of all γ' grains, and then dividing that area by the entire area, the area fraction was found and this approximately corresponds to both the point and volume fractions.

Results and Discussion

Data were gathered from three blades: a new blade, as well as blades that had run for 1891 hours and 10500 hours in the factory test engine. Two trailing edge images were analyzed from each of the three blades. Each image was overlaid with a grid and evaluated via the point counting method and then studied within the platform of the UTHSCSA Image Tool in order to measure the area fraction of γ'. By these two methods, the volume fraction of the γ' phase was determined for each image and blade. **(Table 2)**

With these particular data, however the reduction in the volume fraction of the γ' phase does not appear to show a relationship to the temperature that the blades ex-

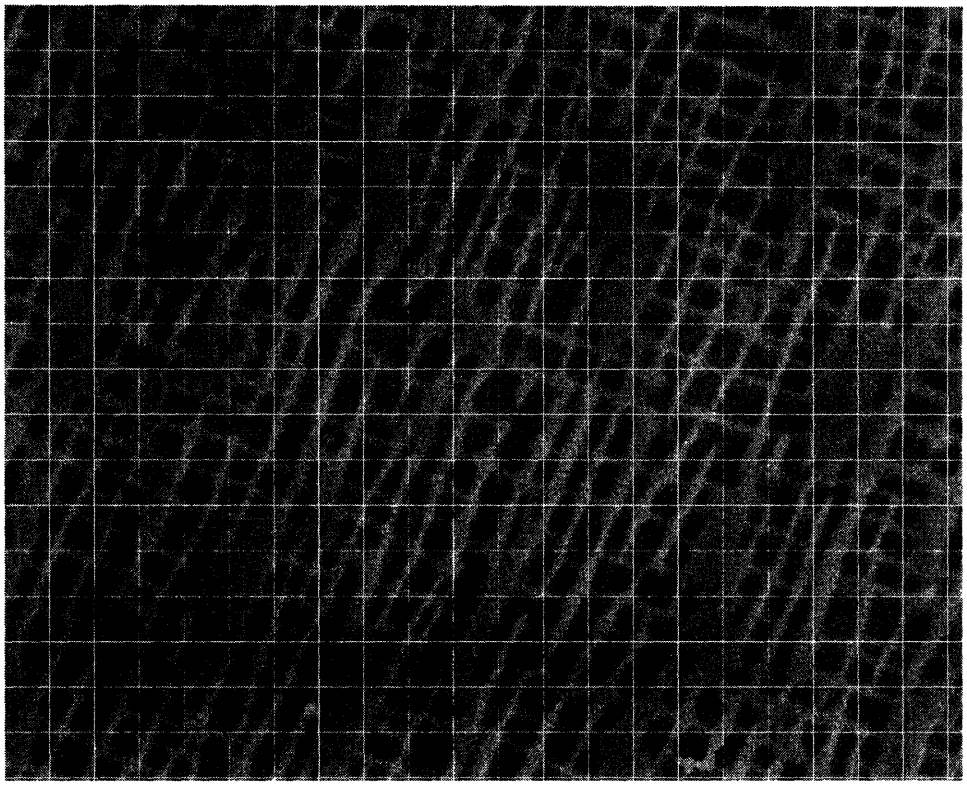

Figure 7: Calculating the γ' volume fraction using the point counting method

perienced. The point counting data did not correlate well to area measurements, and neither data set shows a trend toward lower volume fractions in the run versus unrun blades. Due to this poor data correlation, the temperature cannot be determined by this method.

There are several reasons that the γ' volume fraction would not appear to be reduced in higher temperature blades. The most obvious is that the blades may not have had identical microstructures to begin with. The blade that ran for 1891

Image	Point Counting Method γ' Volume Fraction	Area Measurement γ' Volume Fraction	Average γ' Volume Fraction	Average (per blade) γ' Volume Fraction
New Blade Image 1	49%	38%	43.5%	43.50%
New Blade Image 2	40%	47%	43.5%	
1891 hr. Blade Image 1	53%	54%	53.5%	51.25%
1892 hr. Blade Image 2	44%	54%	49.0%	
10500 hr. Blade Image 1	39%	37%	38.0%	43.25%
10501 hr. Blade Image 2	48%	49%	48.5%	

Table 2: γ' Volume Fraction Data

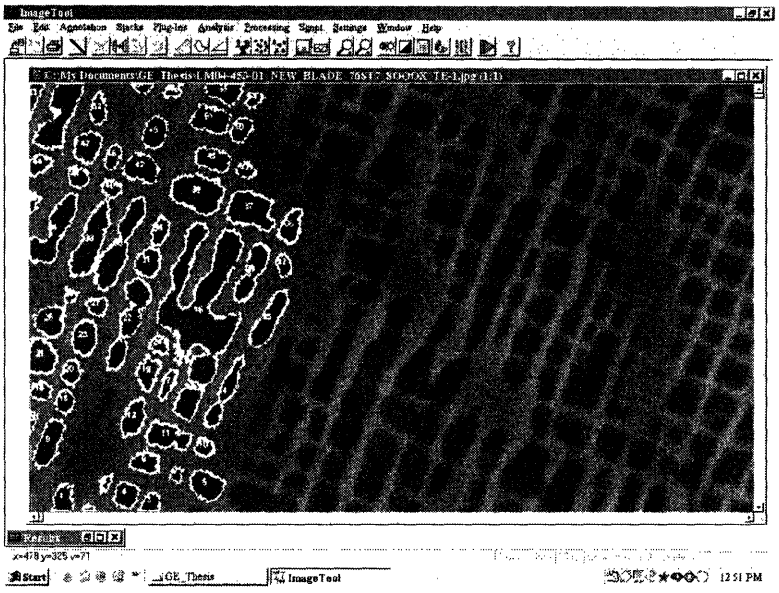

Figure 8: Calculating the γ' volume fraction using Image Tool [13]

hours consistently shows more γ' phase than either of the other blades; this could lead to the conclusion that it began with higher levels of γ' formation than the other two blades. It is also possible that during sample preparation and testing, the volume fraction was altered or misjudged. For example, the etchant used to reveal the microstructure may have preferentially removed one of the phases skewing the results. It could also be something as simple as the quality of SEM images used for this research. Perhaps their quality was simply inadequate to accurately perceive the volume fraction changes. The fuzziness of the images made the analyzing process difficult during both point counting and area measurement. Obtaining better results would require having more blades to average over, having higher quality images to measure, and having a variety of etchants to experiment with to find one that did not distort the volume fractions of either phase.

Coating and Base Material Interdiffusion

Background

Protective coatings were introduced to shield the surface of HPT blades from the high temperature environment. Platinum aluminide coatings are often employed for their oxidation and sulfidation resistance. Their application requires two steps, first the platinum is electrolytically plated onto the substrate. The blade is then heat treated to diffuse the platinum into the base metal [15]. Next the aluminum is applied, often via chemical vapor deposition which produces a finished coating between five and ten thousandths of an inch, that is ductile and has superior thermo-mechanical fatigue properties [22].

A platinum aluminide coating has a three layer structure. **(Figure 9)** As discussed earlier, the platinum plating has diffused into the base metal and then the aluminum reacts with the platinum nickel mixture [16]. At the coating surface, the nickel concentration is low and the platinum and aluminum form a body centered cubic β (beta) phase of the form PtAl. The next two layers likely contain both β and γ' phases; the percentage of β phase lowering from near 100% in the outer coating layer to near 0% in the base material. The difference between the two inner coating layers is the presence of increased levels of heavy element components such as tantalum and tungsten in the layer adjacent to the base material [16].

As a blade is held at elevated temperatures during engine operation, the three distinct coating layers begin to transform. Interdiffusion occurs between the coating elements and the base material elements. The amount of interdiffusion found in a blade depends on how long the blade operated in the engine and at what average temperature.

Materials and Methods

Interdiffusion data were gathered from the same blades and mounted samples as were used for the γ/γ' volume fraction measurements. The samples were examined via

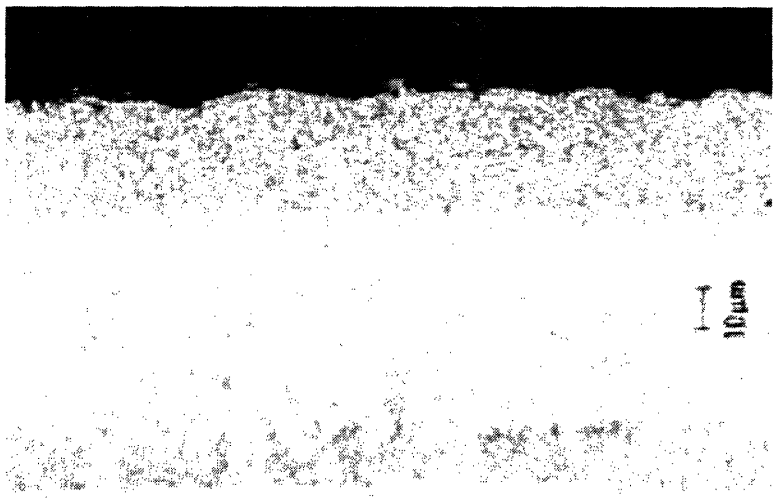

Figure 9: Platinum Aluminide coatings separate into three layers [14]

scanning electron microscopy and EDAX elemental line scan analysis. Line scans were performed beginning at the coating surface and extending substantially into the base material. Analysis was done for nine elements, including all the major components of RENÉ N5® and the platinum and aluminum from the coating.

The line scan data were first correlated to the appropriate elemental compositions in the base material. The weight percentages of each of the elements in the base material portion of the new blade line scan matched well with the expected percentages in **Table 1** except for one element. The weight percentage of aluminum which should be present in the base material is 6.2%; the EDAX results, however, showed approximately half of that amount. **(Figure 10)**

Upon consultation, it was determined that the inaccuracy of the aluminum content was probably the result of preferential etching of the aluminum which distorted the results. Increasing the aluminum percentage by a factor of two across the line profile data was considered an appropriate action to correct for the distortion. Since the EDAX program automatically increased the percentages of all the elements in order to sum to 100%, this must also be accounted for.

Next, the data were used to verify the identity of each layer of the coating and

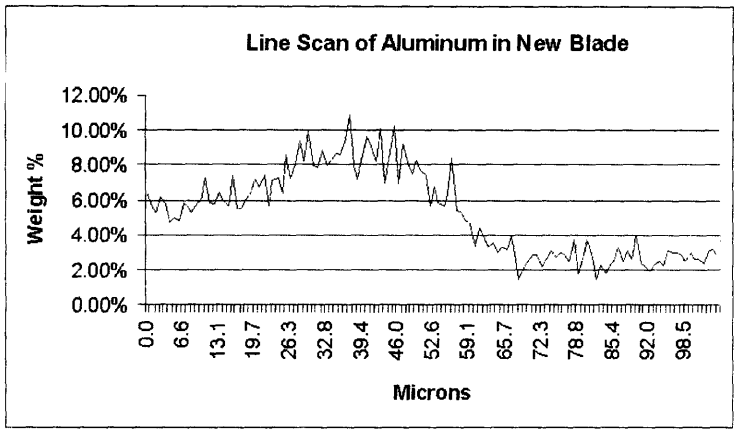

Figure 10: Weight percent line scan of aluminum in the new blade shows too little aluminum in the base material

base material. The atomic percent of aluminum-like elements was compared to the atomic percent of the nickel and nickel-like elements. An element was considered aluminum-like or nickel-like depending on its β and γ' forming abilities. The relative amounts of aluminum-like elements and nickel-like elements in each layer were used to determine which phases were most likely present.

The desired end result of the study was to determine the average temperature at which the blades ran. Therefore, at this point the examination began to focus on the data from the 1891 hour and 10500 hour blades because the new blade would not have experienced engine temperatures. Analyzing the line scan data, it was concluded that the coating and base metal system could be thought of as consisting of three zones: a β coating zone at the surface, a γ plus γ' zone in the base metal, and, in between, a interdiffusion zone of β plus γ'. Before the blade had been subjected to the high temperatures of engine operation, the interdiffusion zone was relatively small. As the material spent time at higher temperatures, the coating and base material elements began to mix and the thickness of the interdiffusion zone increased. This progression of interdiffusion could then be used to estimate the average temperature at which the blade was run.

Given that there are relatively few aluminum-like elements contrasted to many nickel-like elements, it was decided to focus on how aluminum-like elements diffused

in the system. Since the base material was primarily composed of nickel, and the interdiffusion was occurring in a region composed of β phase, the complex interdiffusion of the aluminum-like elements was approximated as the diffusion of aluminum, the main aluminum-like element, in AlNi β phase.

The diffusion of the aluminum-like elements was modeled by an error function solution to Fick's Second Law [21]. **(Equation 1)**

$$\frac{C(x,t) - C_0}{C_s - C_0} = \left[1 - \text{erf}\left(\frac{x}{2\sqrt{Dt}}\right)\right] \tag{1}$$

The compositions are measured in atomic percent. $C_{x,t}$ is the amount of aluminum present at a given distance, x, from the coating surface measured in meters after t seconds of diffusion. C_o and C_s are the percentages of aluminum in the base metal and coating respectively. Diffusivity, D, measured in m^2/s is the only unknown variable. The 1891 hour and 10500 hour blades were analyzed separately. A spreadsheet was formed that calculated, for each position along the line scan, the value of each side of **Equation 1** individually, assuming an initial trial value for the diffusivity. Any difference, δ, between the two sides of the equation was evidence that the trial diffusivity value was not correct. Using an interative method, a value was determined for the diffusivity that minimized δ.

Upon calculating the probable diffusivities for each of the two engine-run blades this information was used to find the average running temperature. Published Arrhenius lines showing diffusivity of aluminum in AlNi with respect to temperature were used to evaluate the blades' average running temperatures based on the calculated diffusivities.

Results and Discussion

Verification of Layer Identities

The identities of the layers present in the platinum aluminide coating and RENÉ N5® base materials can be verified by looking at the elemental compositions in each region. **Figure 11** shows the line scans, in atomic percent, of the sums of the

aluminum-like and nickel-like elements in the new blade. The aluminum percentage has been increased by a factor of two, and the nickel-like element percentage has been decreased accordingly, so that they will sum to 100%.

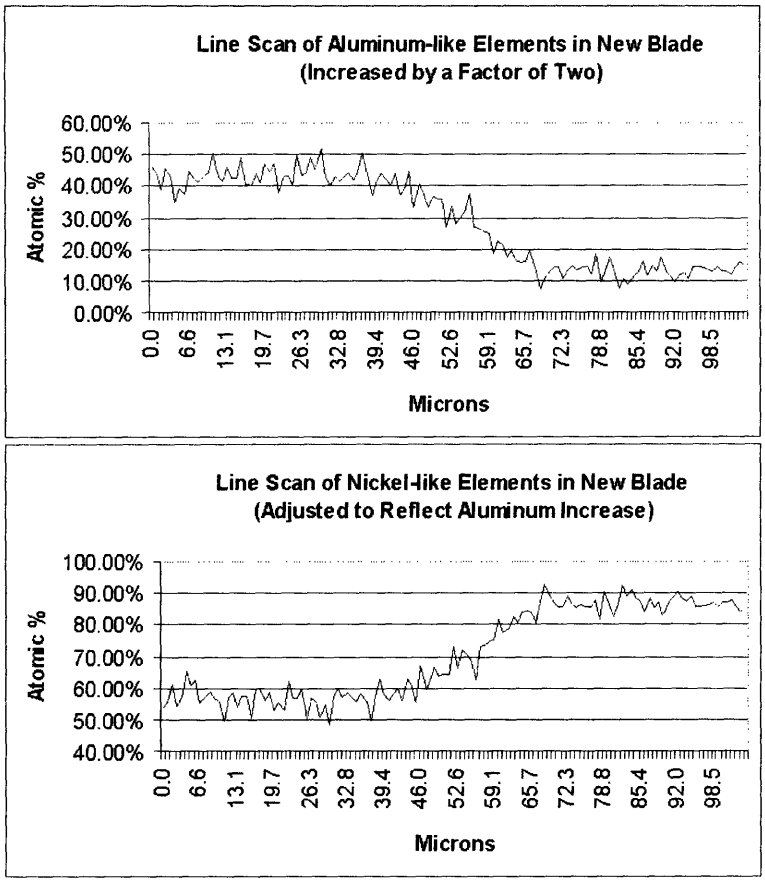

Figure 11: Atomic Percent Line Scans of Aluminum-like and Nickel-like Elements

To the left of the scan is the coating surface. Here there is approximately one half aluminum; this corresponds well to the hypothesis that this is a β phase layer. To the far right of the scan is the base material which should be a γ plus γ' microstructure. The γ' phase would have approximately 25 atomic percent aluminum in it. The γ phase, as seen in **Figure 12**, could have an aluminum percentage up to 15 atomic percent. As seen in the **Table 2** the volume of γ' in each of the blades is approximately 50 percent. This means that the atomic percentage of aluminum in the base material

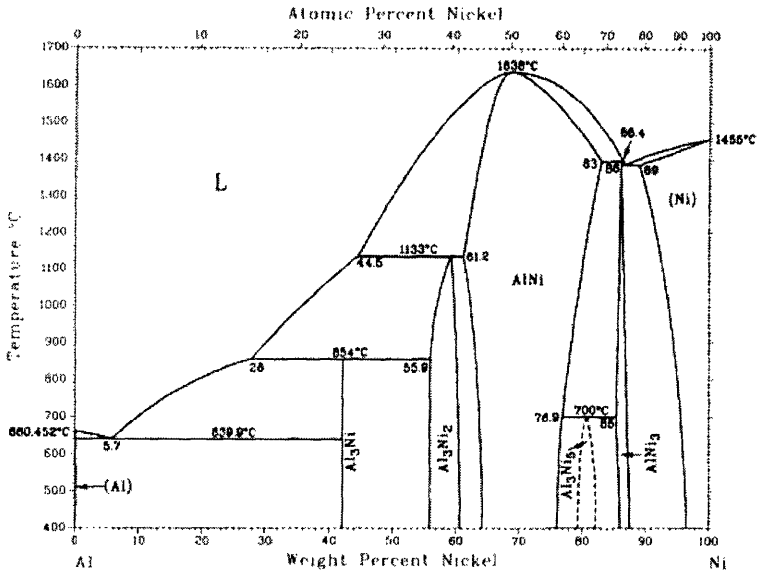

Figure 12: Aluminum-Nickel Binary Phase Diagram [1]

should be the average of 15% and 25% , or 20%, which is what the data show.

The region between the β and γ plus γ' layers, is identified as a β plus γ' layer primarily because of its changing composition. Located as it is, it would be logical for it to either be a single-phase γ or γ' layer or a two-phase β plus γ or γ' layer [8]. The rapidly changing aluminum concentration indicates it is probably not a single-phase layer. The fact that the atomic percentage of aluminum remained closer to 25% before blending into the γ plus γ' region as opposed to dropping to the lower percentage expected in γ indicates that the layer is probably a mix of β (decreasing as it moved toward the base material) and γ'.

Error Function Diffusion Modeling

Figure 13 shows the line scans for the aluminum-like elements in the new blade as well as the 1891 hour and 10500 hour blades. The three regions, β, β plus γ' and γ plus γ' are marked. It can be seen that the β plus γ' interdiffusion zone gets thicker as the blade is run.

Using representative distance and atomic percentage data from the 1891 hour blade, **(Equations 2 - 5)** show an example of how the diffusivities for the systems

were found.

$$\frac{C(x,t) - C_0}{C_s - C_0} = \left[1 - \text{erf}\left(\frac{x}{2\sqrt{Dt}}\right)\right] \tag{2}$$

$$\frac{34.4\% - 18\%}{50\% - 18\%} = \left[1 - \text{erf}\left(\frac{5.05\text{E}^{-8}\,\text{meters}}{2\sqrt{D \times 6807600\,\text{seconds}}}\right)\right] \tag{3}$$

Assuming a diffusivity of $4.5e^{-16}$ m^2/s

$$48.7\% \neq 48.1\% \tag{4}$$

$$\delta = .6\% \tag{5}$$

The final calculated diffusivities for each blade were: $4.5e^{-16}$ m^2/s for the 1891 hour blade and $1e^{-17}$ m^2/s for the 10500 hour blade. These are averaged to $2.3e^{-16}$ m^2/s. Substituting this into the Arrhenius lines in **Figure 14** gives an estimated average running temperature of 1380 K assuming an alloy similar to numbers 4 or 5 in the figure. Compared to the reported average running temperature of 1393 K this shows about a 1% error.

This method of temperature determination was very simplistic. It did not account for the complexities of diffusing through a system composed of 13 elements in varying concentrations. It also did not account for the preliminary diffusion that occurred during the heat treatment. This effect can be seen in the thickness of the diffusion zone in the new blade before it has seen any engine operation.

Conclusions

This thesis attempted to determine the average temperature at which high pressure turbine blades had been run in a test engine. The research was done at GE Aircraft Engines in Lynn, MA on RENÉ N5® HPT blades with a platinum aluminide coating. Three blades were studied: a new blade, one that had run for 1891 hours and one that had run for 10500 hours. The testing as all done at 1393 K.

Two methods were tested as means of temperature determination. The first was

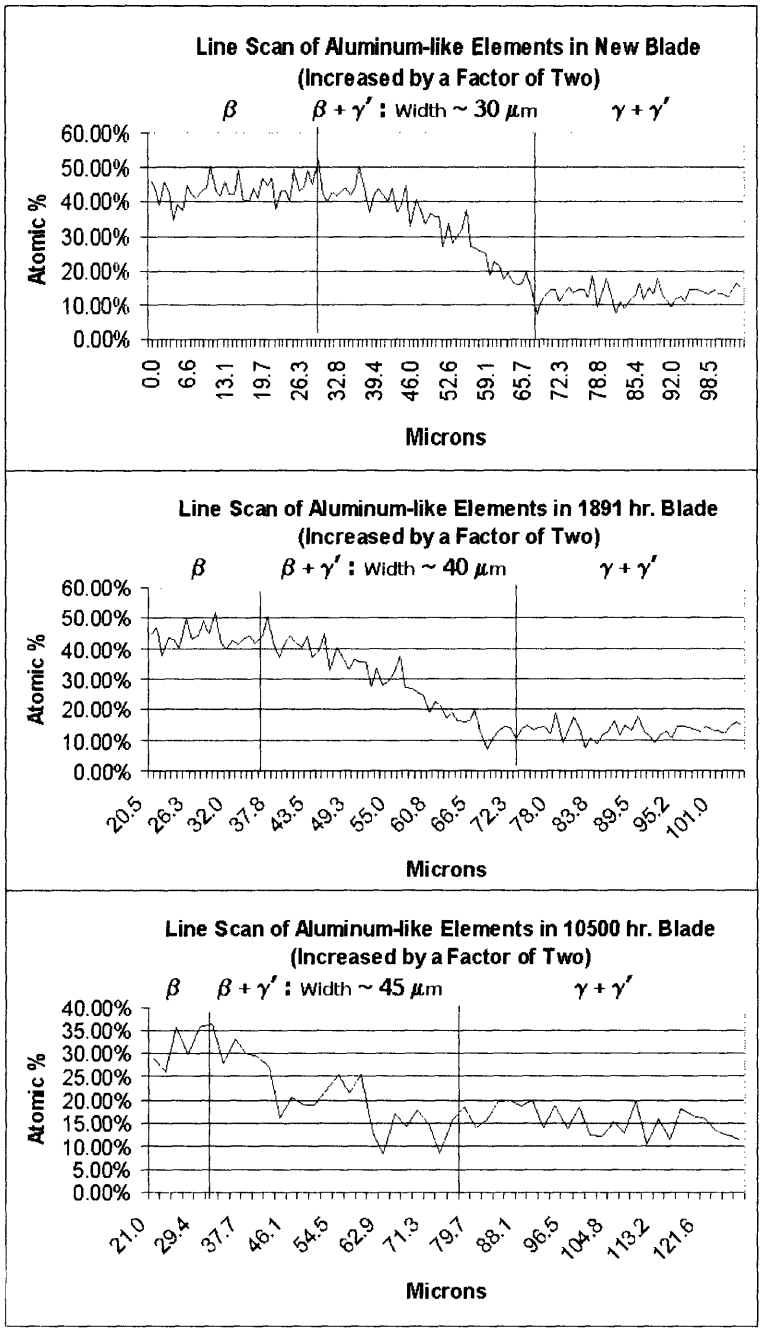

Figure 13: Atomic percent line scans for the aluminum-like elements in all studied blades show the growth of the interdiffusion layer

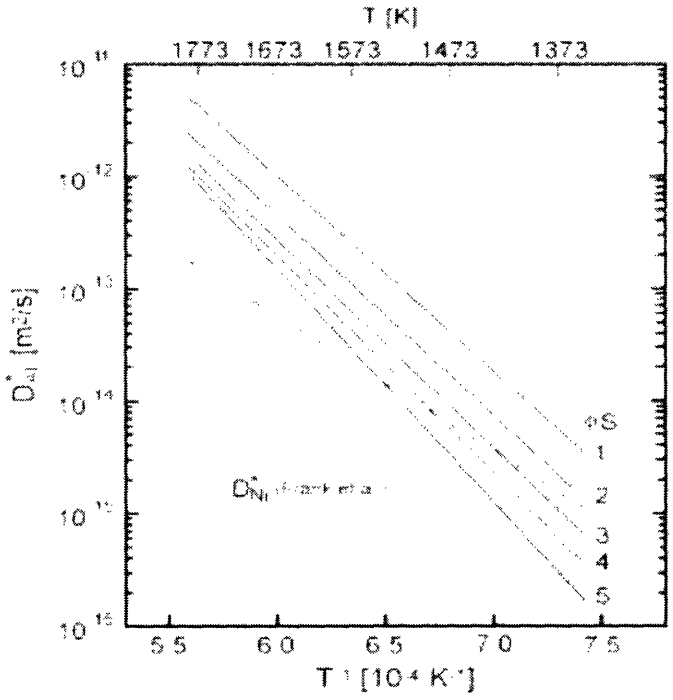

Figure 14: An Arrhenius diffusivity plot for Al in NiAl can be used to estimate an average operating temperature from measured concentration profiles [9]

analysis of the volume fraction of γ' phase in the γ plus γ' microstructure of the base material; this method proved unsuccessful. The second was an error function model of the diffusion of the aluminum-like elements. The interdiffusion method produced an average temperature that was comparable to the actual temperature.

Bibliography

[1] *Alloy Phase Diagrams / prepared under the direction of the ASM International Handbook Committee*, volume 3 of *ASM handbook*. ASM International, Materials Park, OH, 1992.

[2] H. K. D. H. Bhadeshia. Nickel based superalloys. 2003. Available from: `http://www.msm.cam.ac.uk/phase-trans/2003/Superalloys/superalloys.html` [cited February 5, 2005].

[3] Jane Blackford. Engineering of superalloys. Available from: `http://www.cmse.ed.ac.uk/AdvMat45/SuperEng.pdf` [cited November 22, 2003].

[4] General Electric Company. *Seven Decades of Progress: A Heritage of Aircraft Turbine Technology*. Aero Publishers, Inc., Fallbrook, California, 1979.

[5] Lloyd A. Cooke. Life extending advanced component repairs - field operating experience. 2002. Available from: `http://www.liburdi.com/web_pages/tcs_adcomprefurb.shtml`.

[6] A. W. Dix. Materials and process selection for aircraft engine applications: Theory and practice. GE Aircraft Engines, Lynn, Massachusetts, 2003.

[7] B. Gleeson et al. Interdiffusion behavior in an alimunide coated nickel-base alloy at 1150°C. *Elevated Temperature Coatings: Science and Technology IV*, pages 119–132, 2001.

[8] J. E. Morral et al. Modelling the interdiffusion of high temperature coatings. *Elevated Temperature Coatings: Science and Technology II*, pages 245–253, 1996.

[9] Ryusuke Nakamura et al. Single-phase interdiffusion in the B2 type intermetallic compounds NiAl, CoAl and FeAl. *Intermetallics*, (10):195–204, 2002.

[10] T. M. Pollock et al. Creep deformation and the evolution of precipitate morphology in nickel-based single crystals. *Microstructure of High Temperature Materials*, (3):193–212, 1999.

[11] Wukusick et al. Property-balanced nickel-base superalloys for producing single crystal articles. Patent 6074602, United States Patent and Trademark Office, Jun 2000.

[12] Geocities. Principles of jet operation. Available from: `http://www.geocities.com/nedu537/turbine/` [cited November 23, 2003].

[13] University of Texas Health Science Center at San Antonio. Available from: `http://ddsdx.uthscsa.edu/dig/itdesc.html`.

[14] T.A. Kircher, B.G. McMordie, and K. Richards. Use of experimental designs to evaluate formation of aluminide and platinum aluminide coatings. *Surface and Coatings Technology*, 108-109:24–29, 1998.

[15] Liam O'Neill. Platinum plating of gas turbine components. *The Irish Scientist*, 2000. Available from: `http://www.irishscientist.ie/2000/contents.asp?contentxml=079s.xml&contentxsl=insight3.xsl` [cited October 28, 2003].

[16] David Punola, Daniel Sikkenga, and Michael Sutton. Platinum-aluminide coating enhances durability. *Advanced Materials & Processes*, 12 1995.

[17] C. W. Smith. *Aircraft Gas Turbines*. General Electric Series. John Wiley & Sons, Inc., New York, New York, 1956.

[18] M. J. Starink and R. C. Thomson. Modelling microstructural evolution in conventionally cast Ni-based superalloys during high temperature service. *Microstructure of High Temperature Materials*, (3):357–371, 1999.

[19] Y. Tamarin. *Protective Coatings for Turbine Blades.* The Materials Information Society, Materials Park, Ohio, 2002.

[20] Baird Micro Turbines. Turbines. Available from: `http://www.bairdtech.com/bmt/images/turbine.jpg` [cited November 20, 2003].

[21] Dave VanAken. Engineering concepts: The error function and carburization. *Industrial Heating*, 2000. Posted 12-11-2000. Available from: `http://www.industrialheating.com/CDA/ArticleInformation/features/BNP__Features__Item/0,2832,16270,00.html`.

[22] Bruce M. Warnes. Cool coatings let engines run hotter. *Machine Design.* Available from: `http://www.machinedesign.com` [cited November 12, 2003].